ELSEVIER

Ceramics International 26 (2000) 271–277

CERAMICS INTERNATIONAL

Mechanical activation of the synthesis reaction of $BaTiO_3$ from a mixture of $BaCO_3$ and TiO_2 powders

C. Gomez-Yañez, C. Benitez, H. Balmori-Ramirez*

Department of Metallurgical Engineering, ESIQIE, Instituto Politécnico Nacional, A.P.75-593, México City 07738, Mexico

Received 2 February 1999; received in revised form 7 March 1999; accepted 13 May 1999

Abstract

The influence of long term milling in an attritor of a mixture of $BaCO_3$ and TiO_2 powders on the reaction synthesis of $BaTiO_3$ was studied. Thermal analysis (TG and DTA) of the unmilled and milled powders and X-ray diffraction of powders calcined at different temperatures were undertaken. Milling does not change the reaction sequence between $BaCO_3$ and TiO_2. $BaTiO_3$ and Ba_2TiO_4 are produced in both kinds of powders. However, milling reduces the formation temperature and accelerates the formation rate of these two phases. The production of final $BaTiO_3$ is incomplete in the milled powder, probably because of the formation of big crystals of Ba_2TiO_4. As a consequence, the milled powder contains large amounts of Ba_2TiO_4 after calcination at 1200°C. Milling produces allotropic transformations in TiO_2 from anatase phase, to α-PbO_2-like phase and finally to rutile structure.

Keywords: A. Powders: solid state reaction; D. $BaTiO_3$

1. Introduction

$BaTiO_3$ is an important material for the electronic industry. With this material, high capacitance capacitors, thermistors, and humidity and piezoelectric sensors can be made. Traditionally, $BaTiO_3$ has been produced as a product of the reaction between $BaCO_3$ and TiO_2 powders [1]. In order to make this reaction efficient, good homogeneity in the mixture and small particle size of the reactants are desirable. Hence, long-term milling appears to be a good technique to improve the production of $BaTiO_3$. Besides, long-term milling of mixtures of powders has recently demonstrated the feasibility to obtain solid solutions from elements that are not miscible at normal conditions [2], amorphous phases [3], nanocrystalline materials in metallic and non-metallic systems [4], and chemical reactions during the process [5]. Several investigations have been carried out in order to obtain $BaTiO_3$ by mechanically activating the reactants. $BaTiO_3$ resulted from the milling of $BaO + TiO_2$ in a ball mill during 100 h [6], however high temperature treatments were needed to preserve the BaO in pure state, prior to the milling. The milling in a planetary mill of $Ba(OH)_2{\cdot}8H_2O + TiO_2$ resulted in a $BaTiO_3$ powder which had poor crystallinity so an annealing treatment was necessary [7]. Milling of a mixture of powders of $Ba + Ti$ followed by an oxidation heat treatment in an atmosphere of pure oxygen gave also $BaTiO_3$ as product [8].

In continuing these efforts, the purposes of the present work are to analyze the effect of long-term milling on the structure and chemical behavior of the $BaCO_3$ and TiO_2 as reactant powders, and to diminish the temperature of the general reaction:

$$BaCO_3 + TiO_2 \rightarrow BaTiO_3 + CO_2 \quad (1)$$

2. Experimental procedure

A mixture of 55.7 g of $BaCO_3$ (Monterrey, Mexico) and 22.5 g of TiO_2 (Merck) was milled in an attritor (Szegvari, Union Process) using a stainless steel container and milling media (3 mm diameter balls). Both reactants were 99% pure and the weights correspond to the stoichiometric composition of $BaTiO_3$. The sample/

* Corresponding author. Tel.: +52-729-6000; fax: +52-729-6000.

0272-8842/00/$20.00
PII: S0272-8842(99)00053-X

media ratio was 1:36. During milling, samples of about 1 g were taken out at different times. In order to keep the sample/media ratio constant, a fresh powder mixture was added to replace each sample extracted out of the mill. Also, 78.2 g of the same TiO_2 powder used in the mixture were milled up to 78 h. The purpose of this milling was to differentiate between the effect of milling on TiO_2 and the effect due to the presence of $BaCO_3$ during milling.

The unmilled and milled powders were examined by wet chemical analysis methods to identify any possible contamination from the mill, X-ray Diffraction (XRD) (Shimadzu XD-3A, Cu-K_α radiation), simultaneous thermogravimetric analysis (TG) and differential thermal analysis (DTA) (Setaram TG/DTA 92) in air using a platinum crucible (two runs were carried out for each sample) and Scanning Electron Microscopy (SEM) (JEOL JSM–35CF). In order to identify the thermal events recorded in the TG/DTA patterns, several calcinations were performed according to Table 1. Around 3 g of sample were placed in a platinum crucible and heated at 10°C/min in air. The calcined powders were examined by XRD.

3. Results

3.1. Influence of milling on the characteristics of the powders

Chemical analysis indicated 0.012% wt of Fe in the unmilled mixture and 0.096% wt in the powders milled for 72 h. No chromium was detected. Therefore, the contamination by the milling media and the mill was marginal.

The XRD patterns of the $BaCO_3 + TiO_2$ mixture as a function of milling time are shown in Fig. 1. The peaks that appear at 25.15, 37.66, 38.44, and 47.98° correspond to the anatase phase of TiO_2. All the other peaks belong to the whiterite phase of $BaCO_3$. It can be observed in Fig. 1 that the intensity of the TiO_2 peaks decreases when the milling time increases in such a way that after 72 h of milling, only the most intense anatase-TiO_2 peak ($2\theta \sim 25.15°$) remains. The intense peak observed at 2θ 23.8° in the diffraction pattern of the as-received powder corresponds to the reflection (111) of $BaCO_3$. This peak has a shoulder that comes from (021) $BaCO_3$. These two peaks could not be resolved with the equipment used. In the milled powder, the (111) peak decreases and broadens; also, the shoulder becomes confused with the (111) peak. The $BaCO_3$ peaks located at 2θ higher than 30° disappear, overlap or broaden when the sample is milled. These changes indicate particulate size reduction and lattice distortion.

A sample of TiO_2 powder was milled at different times to understand the influence of milling on this compound. The corresponding XRD patterns are presented in Figs. 2 and 3, where it can be observed that the intensity of the TiO_2-anatase peaks decreases due to the milling and almost disappear after milling for 78 h (Fig. 3). Moreover, it is possible to see in Figs. 2 and 3, that new peaks appear after milling, and that their intensity increases with respect to the anatase peak as the milling time increases. The new peaks correspond to rutile-TiO_2, except the peak at $2\theta \sim 31.5°$ which has been reported as belonging to an orthorhombic α-PbO_2-like phase [9,10]. This phase is probably brookite, since the peak at ~31.5° corresponds to such phase of TiO_2, which also has an orthorhombic symmetry [11]. After

Table 1
Calcination treatments for unmilled and milled powders

Samples	Dwell time and temperature	
	5 min, then quenched in air	1 h (cooling rate: 20°C/min)
Unmilled powders	700, 850, 980, 1100, 1200 and 1400°C	1050, 1200°C
Milled powders (72 h)	700,850, 980, 1100 and 1400°C	950, 1200°C

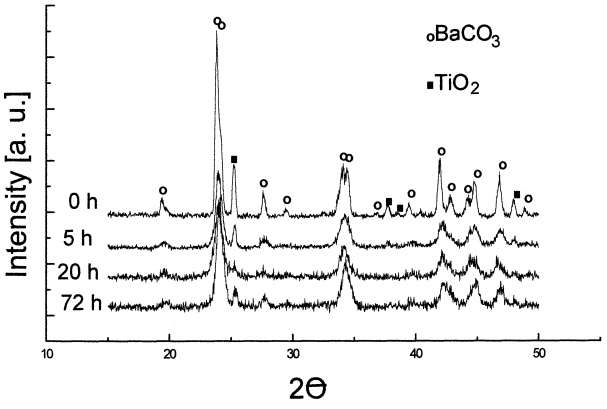

Fig. 1. XRD patterns of the unmilled and milled $BaCO_3 + TiO_2$ mixture.

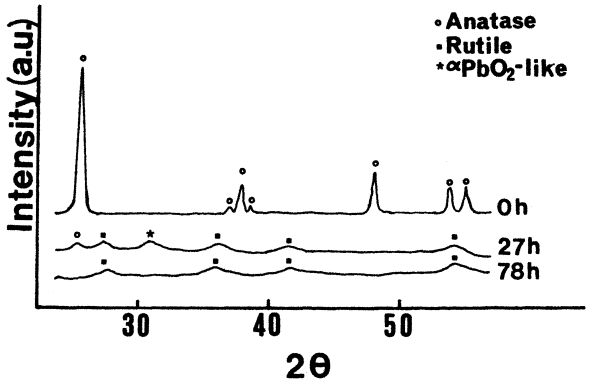

Fig. 2. XRD patterns of unmilled and milled TiO_2 powder.

78 h of milling, the rutile peaks are dominant in the pattern. Examination of Fig. 1 indicates that after milling for up to 72 h the $BaCO_3 + TiO_2$ mixture, the anatase peaks are still there and that rutile and brookite phases could not be detected. There is probably a screening effect of the $BaCO_3$ particles since these particles absorb part of the mechanical energy provided by the collisions of the milling media.

The morphology of the unmilled particles can be observed in Fig. 4a. The needles of about 1 μm length are $BaCO_3$ particles whereas the rounded ones of about 0.2 μm of diameter are TiO_2 particles. It is observed in Fig. 4b that the needle shape of the $BaCO_3$ particles disappeared completely after 72 h of milling and that the mixture of powders is agglomerated.

3.2. Thermal analysis (TG and DTA)

The TG patterns for the unmilled and milled $BaCO_3 + TiO_2$ mixtures are shown in Fig. 5. The curves are drawn at the same scale, but they are shifted on the vertical axis in the sake of clarity. Three thermal events (A, B and C) involving weight loss are distinguished in the milled samples. The TG pattern of the unmilled powder clearly displays two thermal events. However, during the course of the first thermal event there is a change of slope at around 937°C (marked as B) so that, for this powder, three thermal events involving weight loss also occur. The weight loss of the milled powder finishes at a lower temperature, although milling does not change the total weight lost (~15%) with respect to the unground powders. This magnitude of the total weight loss is in accordance with that expected from reaction (1). The proportional weight lost during event C is presented in Table 2 for the unmilled and milled powders. The weight lost during this thermal event is around twice larger in the milled powders than in the unmilled powders.

The DTA patterns of the milled and unmilled samples are presented in Fig. 6. The unmilled powder presents

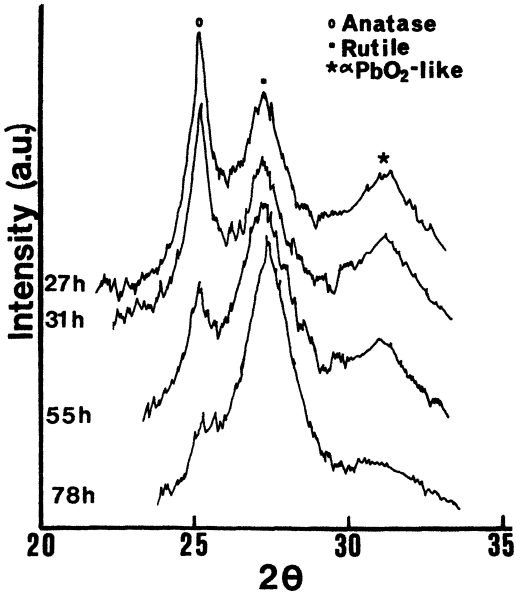

Fig. 3. XRD patterns of milled TiO_2 powder.

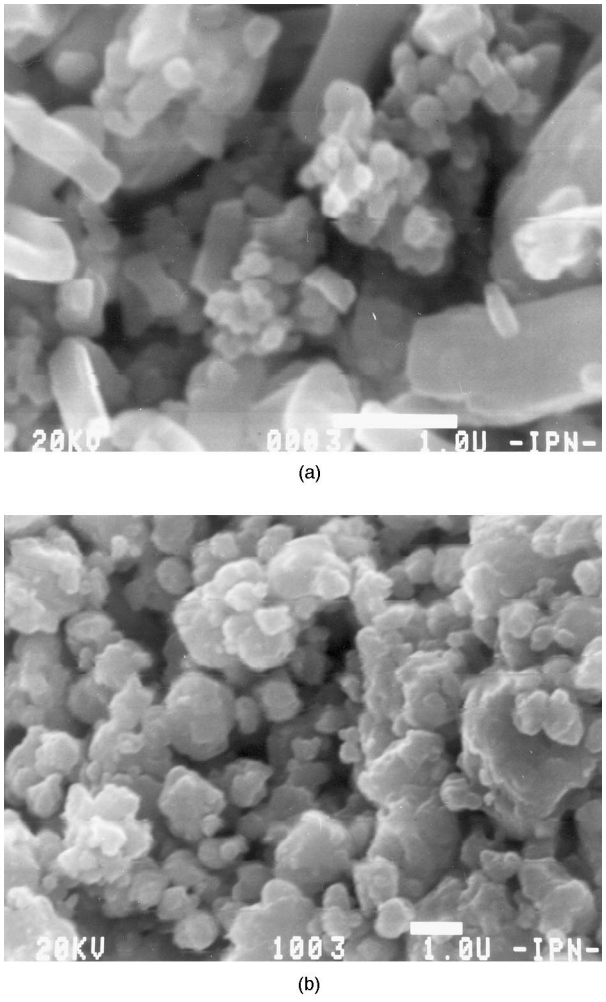

Fig. 4. SEM micrographs of (a) unmilled and (b) 72 h milled $BaCO_3 + TiO_2$ mixture.

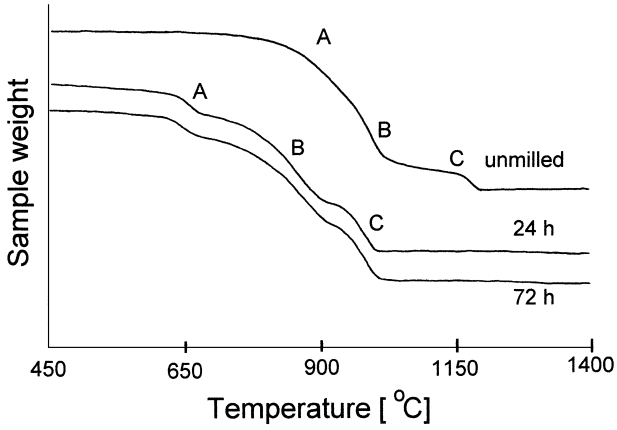

Fig. 5. Thermogravimetric analysis (TG) of unmilled and milled $BaCO_3 + TiO_2$ mixtures.

five endothermic changes, while the milled samples display only three.

Comparison between Figs. 5 and 6 helps to establish the relationship between the TG and DTA curves. A DTA analysis made on pure $BaCO_3$ showed that the peak 1 of unmilled powder coincides with the allotropic transition γ-$BaCO_3 \rightarrow \alpha$-$BaCO_3$ [12]; moreover, this peak is not associated with a weight loss, which is in agreement with this kind of transition. In the unmilled powders, the overlapped TG events A and B correspond to the DTA events 2 and 3, which are also overlapped. The TG event C corresponds to the DTA event 4. The DTA event 5 is not associated with a weight loss. Therefore, it must correspond to a phase transformation or to reaction between solids not involved with any weight change.

In the milled powders, the TG events A, B and C correspond to the DTA events 1, 2 and 3, respectively. The allotropic transition of $BaCO_3$ and the second thermal event (peak 2) occur within the same temperature range. Thus, it is possible that the endothermic peak associated with this transition is overlapped with the phenomena that produces the larger weight loss observed in the TG pattern. Moreover, a hump can be seen between peaks 2 and 3, which suggests that two events were overlapped at around 850°C.

3.3. Calcinations

In order to identify the origin of the thermal events observed in the TG/DTA experiments, several calcinations, followed by quenching, were performed. The XRD patterns of the unmilled powders calcined at different temperatures are shown in Fig. 7. The powder heated up to 700°C only displays the presence of $BaCO_3$ and anatase-TiO_2. The patterns of the untreated powder (Fig. 1) and of the powder calcined at 700°C are similar, except that the later presents better resolved peaks of $BaCO_3$. Broadening and decrease of the reflections of $BaCO_3$ and TiO_2 is observed as the calcination temperature increases, indicating that the calcination produces lattice distortion; reflections of these two species appeared in the XRD patterns until the powders were heated up to 850 and 980°C, respectively. In the powder calcined at 850°C, a broad modulation merges out from the background at around 2θ 31.5°, which becomes a well defined reflection as the heat treating temperature is raised. This peak corresponds to (100) $BaTiO_3$. Other reflections from this phase are observed at higher temperatures. Two small reflections are visible at 2θ 28.6° and 29.2° in the pattern of the powder treated at 1400°C, corresponding to the (211) and (031) reflections of Ba_2TiO_4. It seems that these two peaks developed from the hump observed around the same positions in the patterns of the powders calcined at 980 and 1100°C.

Since the XRD patterns of the powders milled for 5, 20 and 72 h and calcined at different temperatures are similar, only the XRD patterns relevant to the powders milled for 72 h are presented in Fig. 8. The way in which the different phases appear and disappear during the course of the calcinations of the milled and unmilled powders is similar, except for the following differences: In the milled powders calcined at 700°C, the peaks of $BaCO_3$ and TiO_2 are less intense. Also, their reflections disappear faster as the calcination temperature is raised; the peaks of $BaTiO_3$ come out at a lower temperature (700°C) and are better defined. Finally, sharper and more intense reflections of Ba_2TiO_4 are observed, of which a large amount is retained in the milled powder after heating up to 1400°C.

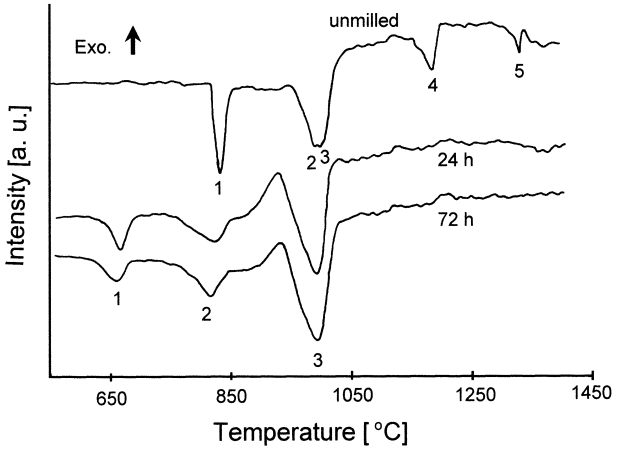

Fig. 6. Differential thermal analysis (DTA) of the unmilled and milled $BaCO_3 + TiO_2$ mixtures.

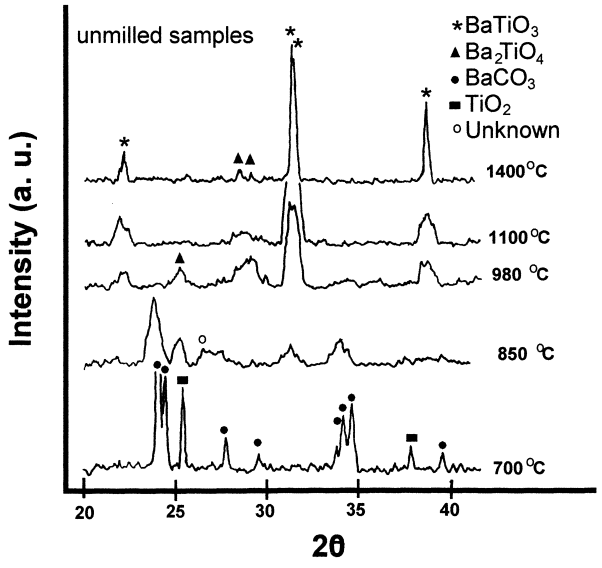

Fig. 7. XRD patterns of unmilled powders calcined for 5 min at different temperatures and quenched in air.

Faint diffraction peaks around 2θ 26.7° are visible in the pattern of the milled powder calcined at 850°C. These peaks do not match with any of the JCPDS diffraction cards available for Ba–Ti–O compounds or barium and titanium oxides [13]. Only the peak at 26.7° coincides with the main reflection of $BaTi_3O_7$ (JCPDS card 38-1482). The formation of this phase during the production of $BaTiO_3$ has been suggested previously [6], but it is not possible to identify it unambiguously in the present work, because other reflections from this phase are not seen. In the unmilled powder (Fig. 7), there is also a broad reflection centered at this position, which might have the same origin as in the milled powder. In both cases, it seems that a transient specie or species produce these peaks because they disappear in the powders calcined at higher temperatures in both kinds of powders.

Fig. 9 shows XRD patterns relevant to the unmilled and 72 h milled powder calcined for 1 h at 1050 and at 950°C, respectively. The diffractograms of the two powders are similar; both show a mixture of $BaTiO_3$ as major component, and intense Ba_2TiO_4 reflections. The morphology of the crystals after calcination is presented in Fig. 10. Long needles can be seen in the sample of the milled powder calcined at 950°C (Fig. 10b), while these needles were not observed in the unmilled sample calcined at 1050°C (Fig. 10a). A semiquantitative Energy Dispersive Spectroscopy Analysis (EDS) showed that the needles have approximately the Ba/Ti compositional ratio of Ba_2TiO_4, so this compound probably composes these crystals.

When the unmilled and the milled samples are treated at 1200°C during 1 h, the XRD patterns of both samples are different (Fig. 11); the XRD pattern of the unmilled sample consists basically of $BaTiO_3$ whereas

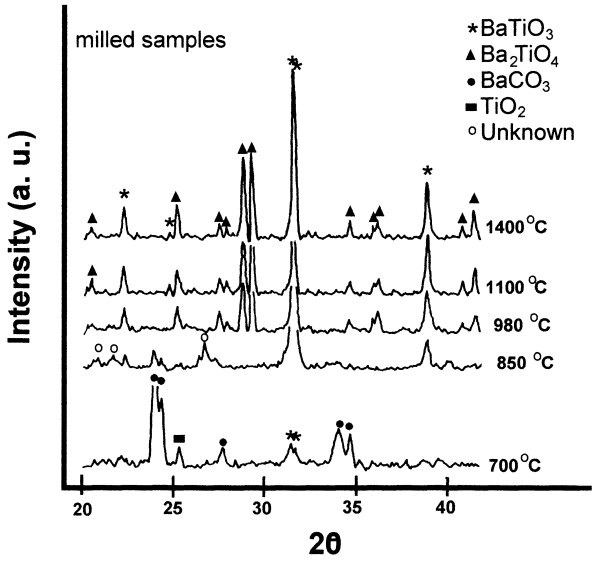

Fig. 8. XRD patterns of milled powders calcined for 5 min at different temperatures and quenched in air.

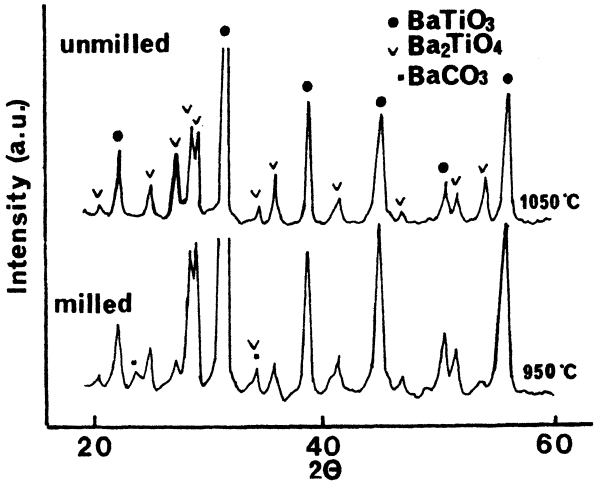

Fig. 9. XRD patterns of calcined powders: (a) unmilled powders calcined at 1050°C for 1 h; (b) milled powders calcined at 950°C for 1 h.

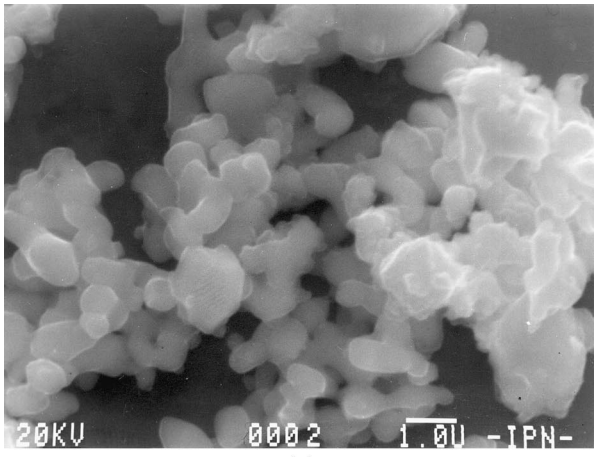

(a)

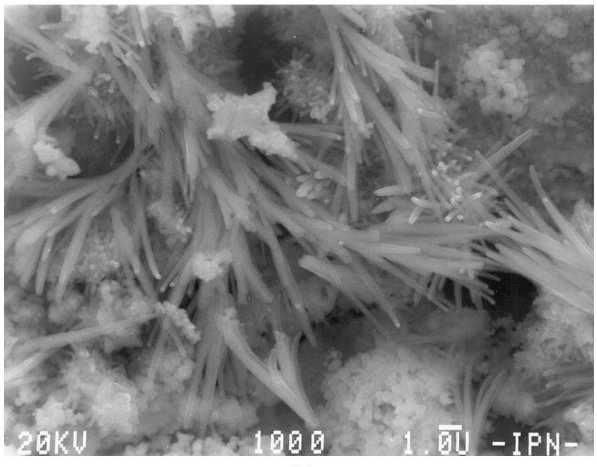

(b)

Fig. 10. SEM micrographs of (a) unmilled powders calcined at 1050°C for 1 h and (b) milled powders calcined at 950°C for 1 h.

the XRD pattern of the milled sample still presents Ba_2TiO_4 and residual $BaCO_3$. EDS examination on both samples verified that the initial average Ba/Ti ratio did not change after milling and calcinations. The results of Figs. 9 and 11 demonstrate that Ba_2TiO_4 forms in the milled and unmilled powders, but that it disappears faster in the unmilled case after calcination at a high temperature.

4. Discussion

The XRD patterns of the unmilled and milled powders calcined at different temperatures show that $BaTiO_3$ and Ba_2TiO_4 are the major phases that appear during the reaction between $BaCO_3$ and TiO_2. In both kinds of powders, $BaTiO_3$ comes out first and it is formed in larger quantities than Ba_2TiO_4. By making a series of isothermal experiments at 900°C, Beauger et al. [14,15] proposed that $BaTiO_3$ and Ba_2TiO_4 are formed as products of the following reactions:

$$BaCO_3 + TiO_2 \rightarrow BaTiO_3 + CO_2 \uparrow \quad (2)$$

$$BaTiO_3 + BaCO_3 \rightarrow Ba_2TiO_4 + CO_2 \uparrow \quad (3)$$

These two reactions are associated with a weight loss owing to the evolution of gaseous CO_2. The TG and DTA results of the unmilled powder show a thermal event involving a weight loss that starts slowly at 700°C and then accelerates as the temperature is raised up to 1031°C. From this point, the weight loss rate slows down and then accelerates again at approximately 1150°C. The loss of weight ends up at 1200°C. These two events correspond respectively to the formation of $BaTiO_3$ according to reaction (2) and of Ba_2TiO_4 according to reaction (3), but the two reactions are overlapped. The beginning of the formation of Ba_2TiO_4 seems to be a slow process in the unmilled powder, as can be deduced from the fact that the thermal event related with it starts slowly and because the XRD patterns shown in Fig. 7 only have small and diffuse reflections related to this compound.

In the unmilled powder, the Ba_2TiO_4 tends to disappear when the calcination temperature increases, as can be seen in the XRD patterns of Fig. 9 and 11. Beauger et al. [14,15] also proposed that a solid state reaction between Ba_2TiO_4 and TiO_2 yields $BaTiO_3$ as a product:

$$Ba_2TiO_4 + TiO_2 \rightarrow 2BaTiO_3 \quad (4)$$

The DTA curve of the unmilled powder displays an endothermic peak (peak 5) that starts at 1280°C, with a maximum reaction rate at 1330°C. Reaction (4) could account for this event, since it is not associated with a weight loss.

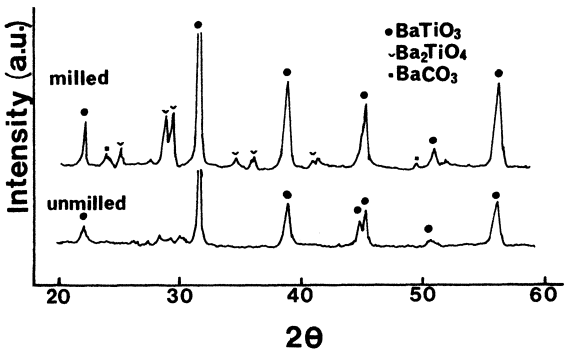

Fig. 11. XRD patterns of the unmilled and milled powders calcined at 1200°C for 1 h.

Table 2
Weight loss during thermal event C

Powder	Weight loss (%) during thermal event C
Unmilled	2.6
Milled for 24 h	4.8
Milled for 72 h	5.6

Reactions (2)–(4) can also be used to explain the changes experienced by the milled powder. The formation of $BaTiO_3$ occurs during the thermal event comprised between 675 and 900°C, marked as B in Fig. 5. The beginning temperature of this event is just slightly lower than in the unmilled powder; it advances faster too. The small thermal event observed at the beginning of the TG curve of this powder, starting at 650°C, could not account for the formation of $BaTiO_3$ because the weight loss connected with it is too small. It is probably associated with the formation of transient phases formed during the course of the reaction and that do not show up in the final products, such as those that give rise to the unidentified peaks observed in the XRD patterns of the calcined powders.

In the milled samples, the formation of $BaTiO_3$ overlaps with a second reaction at 900°C that marks the onset for the formation of Ba_2TiO_4. This event lasts until 1012°C, which is a smaller temperature than in the unmilled powder. The proportion of the total weight lost during this event sums up 4.8 and 5.6% for the powders milled for 24 and 72 h, respectively (Table 2), whereas in the unmilled powder it is of only 2.6%. Furthermore, the corresponding DTA peak of the milled powders is bigger. Hence, a larger amount of Ba_2TiO_4 should have been formed in the milled powders, as can be seen in the XRD patterns of Fig. 8. Consequently, a smaller amount of the other phases such as $BaTiO_3$ should have been formed as well.

The milled powders do not display a DTA event which could account for reaction (4). On the other hand, the XRD patterns taken from the powder calcined at 1400°C (Fig. 8) and of Figs. 9 and 11 display large peaks of Ba_2TiO_4. Consequently, it is apparent that reaction 4 does not occur in the milled powders, or that it is a slow process. Probably, what is hindering the formation of $BaTiO_3$ by reaction (4) in the milled powder, is the production of large amounts of big and well defined Ba_2TiO_4 crystals (Fig. 10b) that could make more difficult the diffusion process necessary for reaction (4) to proceed. Even when a heat treatment at 1200°C during 1 h is applied, Ba_2TiO_4 remains in the powder (Fig. 11).

5. Conclusions

1. Mechanical activation of the synthesis reaction of $BaTiO_3$ from a mixture of $BaCO_3$ and TiO_2 accelerates the formation rate of $BaTiO_3$ and of Ba_2TiO_4. However, it does not change the basic formation mechanism of barium titanate.
2. Intensive milling in an attritor decreases the rate of reaction (4), probably due to the previous production of large Ba_2TiO_4 crystals. Consequently, the milled powders contain a large amount of this phase.
3. Milling provokes phase transformations in TiO_2 powders. After 25 h of milling, the anatase phase transforms to rutile and α-PbO_2-like phases (probably brookite). Furthermore, after 78 h of milling, the anatase and α-PbO_2-like phases disappear almost completely, remaining only the rutile phase.

Acknowledgements

This work was performed under a research project (DEPI-951196) granted by the Instituto Politécnico Nacional.

References

[1] J.M. Herbert, Ceramic Dielectric and Capacitors, Gordon and Breach Science Publishers, London, 1985.
[2] S. Diaz de la Torre, Metastable alloy phase formation in immiscible metallic systems produced by mechanical alloying, Ph.D. thesis, Department of Energy Science and Engineering, Kyoto University, Japan, 1995.
[3] J.G. Cabañas-Moreno, V.M. Lopez-Hirata, Mater. Trans. JIM 36 (1995) 218–227.
[4] K.J. Kim, K. Sumiyama, K. Suzuki, J. Non-Cryst. Solids 168 (1994) 232–240.
[5] V.V. Boldyrev, N.Z. Lyakhov, Y.T. Pavlyukhin, E.V. Boldyreva, E.Y. Ivanov, E.G. Avakumov, Sov. Sci. Rev. B Chem. 14 (1990) 105–155.
[6] N.J. Welham, J. Mater. Res. 13 (1998) 1607–1613.
[7] O. Abe, Y. Suzuki, Mater. Sci. Forum 225–227 (1996) 563–568.
[8] M.M. Antony, K.H. Sandhage, J. Mater. Res. 8 (1993) 2968–2977.
[9] J. Chaudhuri, M.L. Ram, B.K. Sarkar, J. Mater. Sci. 29 (1994) 3484–3488.
[10] S. Begin-Colin, G. Le Caer, M. Zandona, E. Bouzy, B. Malaman, J. Alloys and Comp. 227 (1995) 157–166.
[11] E.M. Kostic, S.J. Kiss, S.B. Boskovic, S.P. Zec, Am. Ceram. Soc. Bull. 76 (1997) 60–64.
[12] R.H. Perry, D. Green, Perry's Chemical Engineer's Handbook, McGraw Hill, Tokyo, 1984.
[13] Joint Committee on Chemical Analysis by Powder Diffraction Methods, ASTM, 1995.
[14] A. Beauger, J.C. Mutin, J.C. Niepce, J. Mater. Sci. 18 (1983) 3041–3047.
[15] A. Beauger, J.C. Mutin, J.C. Niepce, J. Mater. Sci. 18 (1983) 3543–3550.